Lawrence Berkeley National Laboratory
LBL Publications

Title

FATIGUE CRACK PROPAGATION IN OIL ENVIRONMENTS: PART I: CRACK GROWTH BEHAVIOR IN SILICONE AND PARAFFIN OILS

Permalink

https://escholarship.org/uc/item/7t93s8vn

Authors

Tzou, J.-L.
Suresh, S.
Ritchie, R.O.

Publication Date

1983-12-01

eScholarship.org Powered by the California Digital Library
University of California

UC-25
LBL-16028
Preprint

Lawrence Berkeley Laboratory
UNIVERSITY OF CALIFORNIA

Materials & Molecular Research Division

RECEIVED
LAWRENCE
BERKELEY LABORATORY
MAY 1 1984
LIBRARY AND
DOCUMENTS SECTION

Submitted to Acta Metallurgica

FATIGUE CRACK PROPAGATION IN OIL ENVIRONMENTS:
PART I: CRACK GROWTH BEHAVIOR IN SILICONE
AND PARAFFIN OILS

J.-L. Tzou, S. Suresh, and R.O.

For Reference
Not to be taken from this room

December 1983

Prepared for the U.S. Department of Energy under Contract DE-AC03-76SF00098

LBL-16028

DISCLAIMER

This document was prepared as an account of work sponsored by the United States Government. While this document is believed to contain correct information, neither the United States Government nor any agency thereof, nor the Regents of the University of California, nor any of their employees, makes any warranty, express or implied, or assumes any legal responsibility for the accuracy, completeness, or usefulness of any information, apparatus, product, or process disclosed, or represents that its use would not infringe privately owned rights. Reference herein to any specific commercial product, process, or service by its trade name, trademark, manufacturer, or otherwise, does not necessarily constitute or imply its endorsement, recommendation, or favoring by the United States Government or any agency thereof, or the Regents of the University of California. The views and opinions of authors expressed herein do not necessarily state or reflect those of the United States Government or any agency thereof or the Regents of the University of California.

LBL-16028

FATIGUE CRACK PROPAGATION IN OIL ENVIRONMENTS:

PART I: CRACK GROWTH BEHAVIOR IN SILICONE AND PARAFFIN OILS

J.-L. Tzou,[1] S. Suresh,[2] and R. O. Ritchie[1]

[1]Materials and Molecular Research Division, Lawrence Berkeley Laboratory, and Department of Materials Science and Mineral Engineering, University of California, Berkeley, CA 94720

[2]Division of Engineering, Brown University, Providence, RI 02912
Formerly Department of Materials Science and Mineral Engineering, University of California, Berkeley, CA 94720

December 1983

This work was supported by the Director, Office of Energy Research, Office of Basic Energy Sciences, Materials Science Division of the U.S. Department of Energy under Contract No. DE-AC03-76SF00098.

FATIGUE CRACK PROPAGATION IN OIL ENVIRONMENTS:

PART I: CRACK GROWTH BEHAVIOR IN SILICONE AND PARAFFIN OILS

J.-L. Tzou, S. Suresh* and R. O. Ritchie

Materials and Molecular Research Division
Lawrence Berkeley Laboratory
and
Department of Materials Science and Mineral Engineering
University of California
Berkeley, CA 94720

Abstract - The influence of dehumidified silicone and paraffin oils with kinematic viscosities varying from 5 to 60,000 cS has been examined on fatigue crack propagation in a lower strength bainitic steel over a range of growth rates from near-threshold levels (10^{-6} to 10^{-8} mm/cycle) to higher growth rates (up to 10^{-3} mm/cycle). Crack growth data for a cyclic frequency of 50 Hz at both low and high load ratios are compared with previous results for environments of moist air, dry gaseous hydrogen and dry gaseous helium. It is found that at low load ratios, growth rates in oil **exceed** those in moist air **below** 10^{-6} mm/cycle, yet are **lower** than in moist air **above** 10^{-6} mm/cycle. Furthermore there is a small but definite trend of higher growth rates in the higher viscosity oils. Such observations are discussed and interpreted in terms of three mutually competitive mechanisms specific to dry viscous environments, namely suppression of moisture-induced hydrogen embrittlement and/or metal dissolution, minimization of oxide-induced crack closure, and the hydrodynamic wedging action of the oil inside the crack. A quantitative analysis for the effect of crack closure induced by a viscous medium is developed in Part II of this paper.

---

*Currently in the Division of Engineering, Brown University, Providence, RI 02912.

1. INTRODUCTION

Recently, there has been considerable interest in the role of crack closure mechanisms in influencing fatigue crack propagation in metals and alloys, and in particular, in the contribution of such mechanisms to microstructural and environmental effects commonly observed at very low growth rates below typically 10^{-6} mm/cycle (for a recent review, see ref. 1). Such closure leads to the suppression of the effective driving force for crack advance through premature contact between the crack surfaces at positive loads during the fatigue cycle such that, under small-scale yielding conditions, the stress intensity range is reduced from the nominally applied value ΔK, computed from applied loads, geometry and crack length measurements, to some lower effective value, ΔK_{eff}, actually experienced at the crack tip.[2] Specifically below 10^{-6} mm/cycle, where growth rates approach a fatigue threshold stress intensity range, ΔK_o, below which long cracks* remain dormant or propagate at experimentally undetectable rates, the origin of such fatigue crack closure is found to be not solely a result of cyclic plasticity,[2,4] as first envisioned by Elber's plasticity-induced closure concept,[2] but additionally from the formation of insoluble crack surface corrosion deposits,[5-12] irregular fracture morphologies coupled with inelastic Mode II crack tip displacements,[13-19] the wedging action of viscous fluids contained within the crack,[20-22] and from metallurgical phase transformations.[1] Such crack closure mechanisms are schematically illustrated in Figure 1.

*Long cracks here refer to cracks of a length large compared to the scale of microstructure or the scale of local plasticity. The distinction is made since short cracks, which are small compared to such size-scales, are known to propagate below the long crack threshold ΔK_o (see, for example, ref. 3).

To date, most closure studies have been exclusive to simple gaseous and aqueous environments, e.g., room air, hydrogen gas, distilled water, etc., where behavior can be modelled to result from a mutual competition between corrosion fatigue processes, e.g., hydrogen embrittlement and active path corrosion, which **accelerate** crack growth, and the accompanying closure mechanisms which **retard** it. Only very seldom, however, have attempts been made to examine the effect of **viscous** environments on fatigue crack growth characteristics[20-25] and in particular whether the presence of a viscous fluid within an extending fatigue crack can induce additional closure through hydrodynamic wedging action.[20-22]

It is the objective of the present work to investigate fatigue crack propagation behavior for a bainitic steel in non-corrosive viscous environments, specifically silicone and paraffin oils, and to examine systematically the role of viscosity changes from 5 to 60,000 cS in influencing crack extension over a wide range of growth rates (i.e., 10^{-8} to 10^{-3} mm/cycle). Through comparison to previous data for this steel in moist air, dry hydrogen and dry helium gas environments,[9,10] fatigue behavior in viscous fluids is discussed in terms of corrosion fatigue and closure mechanisms. The question of closure induced by the wedging action of a viscous fluid is examined in the following Part II of this paper,[26] and a new quantitative model for this closure mechanism is developed based on the fluid pressure resulting either from the partial or full penetration of the oil inside the crack.

2. BACKGROUND

Over the past 45 years there have been numerous studies on the role of oil environments in affecting fatigue life,[20,21,23-43] promoted largely by the problems of rolling contact fatigue in lubricated bearings. The majority of these studies interpret the effect of the oil medium in influencing fatigue behavior simply in terms of suppressing, or in the odd case promoting, some environmental contribution to crack initiation and subsequent growth. For example, several investigations in both ferrous[21-23,27,28] and non-ferrous[20,27] alloys have shown that Stage II fatigue crack growth rates (i.e., typically between 10^{-5} to 10^{-2} mm/cycle) are slower in non-corrosive oils, such as mineral or silicone oils, compared to room air. However, when water is added to such fluids, studies on rolling contact fatigue in lubricated bearing steels have shown that the water greatly accelerates pitting failures leading to significant reduction in surface fatigue life.[27,29-32] In somewhat similar vein, studies on Stage II fatigue crack growth in HSLA pipeline steels tested in sour crude oil have demonstrated that growth rates could be increased by some 3 to 20 times, compared to room air, as the H_2S concentration in the oil was increased from 1 ppm to saturation level (4700 ppm).[24,25]

In addition to the role of oils in providing a non-corrosive environment for fatigue (at least where chemically-active species are not added), many investigations on the fatigue of ball or roller

bearings have reported fatigue lifetimes to be increased,[34-40] decreased[37] or sometimes unchanged[37,41,42] by increasing the viscosity of the oil. In particular, early studies on Stage II crack propagation at constant stress amplitude in tin and copper-lead bearing metals and in a medium carbon steel tested in non-corrosive mineral and polymeric silicone oils indicated that growth rates were **decreased** with increasing fluid viscosity.[20,21] More recent studies, on the other hand, for a low carbon alloy steel tested in similar oils but at higher frequencies (50 Hz) over a much wider spectrum of propagation rates (i.e., $\sim 10^{-8}$ to 10^{-3} mm/cycle) indicated growth rates to be slightly **increased** with increasing viscosity.[22]

The effect of oil viscosity on fatigue behavior has been explained in terms of the fluid penetrating into the crack and creating a hydraulic wedge, but unfortunately the mechanism differs widely in its interpretation. Way,[43] for example, proposes that such fluid penetration, which forms a wedge within the crack, will **increase** crack growth rates by providing an additional driving force for crack advance, and further suggests that this **accelerating** effect will be enhanced in lower viscosity oils due to easier penetration. Endo et al.,[20,21] conversely, interpret essentially the same mechanism to **decrease** crack growth rates through an effect of the hydrodynamic oil pressure, generated by the **complete penetration** of oil into the closing crack, in reducing the effective stress amplitude experienced at the crack tip. Since in their "full penetration" model the internal oil pressure is directly proportional to viscosity, these authors expect

this decelerating effect of the oil to be enhanced in higher viscosity oils.

Clearly, the various mechanisms by which oil environments can affect fatigue behavior have yet to be documented in any systematic way, and further the specific role of fluid viscosity remains largely unresolved. Any quantitative analysis of the latter effect must include considerations of both the hydrodynamic oil pressure created within the pulsating crack walls and the extent of fluid penetration into the crack, processes which will have opposite dependencies on viscosity. One of the objectives of the current work is to develop a model for crack closure induced by a non-reacting viscous fluid by estimating the extent of oil penetration based on simple considerations of capillary flow[20,40,44] and then computing the internal oil pressure for the partially penetrated crack. As shown below and in the companion paper (Part II),[26] such concepts can be used to rationalize the widely contradicting effects reported for the influence of oil viscosity on fatigue behavior.

3. EXPERIMENTAL PROCEDURES

The material used in this study was an ASTM A542 Class 3, 2.25Cr-1Mo steel. Following austenitizing at 954°C, water quenching, tempering 8 h at 663° and stress relieving 15 h at 593°C, 22 h at 649°C, 18 h at 663°C, the microstructure was granular bainite (less than 3 pct polygonal ferrite) with a yield strength of 500 MPa. Chemical composition and room temperature mechanical properties are

listed in Tables I and II, respectively. This particular heat of steel has been the subject of several recent studies where environmentally-influenced fatigue crack propagation behavior has been well-documented.[6,9,10,45,46]

Fatigue crack propagation tests were performed on 12.7 mm thick 1-T compact C(T) specimens, machined in the T-L orientation.* Specimens were cycled under load control, with a cyclic frequency of 50 Hz (sine wave), at load ratios of 0.05 and 0.75 (where load ratio $R = K_{min}/K_{max}$). Using d.c. electrical potential techniques to monitor continuously crack length, thresholds were approached using manual load shedding procedures with the value of ΔK_o defined at a maximum growth rate of 10^{-8} mm/cycle (4×10^{-10} in/cycle), as described in detail elsewhere.[47]

Tests were performed at room temperature in a series of **dehumidified** oils, namely a series of chemically similar silicone oils (dimethyl polysiloxane) of kinematic viscosities ranging from 5 to 60,000 cS and two chemically similar paraffin oils (mixture of saturated aliphatic and naphthentic hydrocarbons) with kinematic viscosities of 25 and 75 cS. The physical properties of these oils are listed in Table III. Testing was achieved by full immersion of the specimen in a stainless steel oil bath clamped to the loading train. The oil was continuously dehumidified **in situ** by bubbling through dry ultrapure helium gas with the whole environmental enclosure sealed to

*Based on the criterion that the cyclic plastic zone size (r_Δ) remained small compared to thickness (B), i.e., $r_\Delta \approx 1/2\pi\ (\Delta K/2\sigma_y)^2 \lesssim 1/15$ B, this geometry was sufficient to maintain plane strain conditions.

maintain a positive pressure of helium, thus minimizing contact with the atmosphere.

Fracture surfaces were subsequently examined in the scanning electron microscope and from Ar^+ sputtering techniques using Auger electron spectroscopy to assess quantitatively the extent of fracture surface oxidation. The latter technique has been described in detail elsewhere.[9,10]

4. RESULTS

Fatigue Crack Growth Data

The variation of fatigue crack propagation rates (da/dN) with nominal stress intensity range ($\Delta K = K_{max} - K_{min}$) for the A542 steel tested in the silicone oil and paraffin oil environments at R = 0.05 is shown in Figs 2 and 3, respectively, and at R = 0.75 in Fig. 4. Results are compared with previous data[9,10] for this steel tested in room temperature moist air (30 pct relative humidity), dehumidified gaseous hydrogen and dehumidified gaseous helium (all at atmospheric pressure). At low load ratios (R = 0.05), crack growth rates in silicone oils are **slower** than those in moist air **above** $\sim 10^{-6}$ mm/cycle, yet **faster** at near-threshold levels **below** $\sim 10^{-6}$ mm/cycle (Fig. 2). Behavior in the paraffin oils is similar, although the increase in growth rates at near-threshold levels and reduction in growth rates above $\sim 10^{-6}$ mm/cycle is somewhat larger (Fig. 3). Threshold ΔK_o values in oil are at least 20 pct lower than in air and comparable to those for dry gaseous environments. At high load ratios (R = 0.75),

thresholds for moist air, hydrogen gas and the various oil environments are virtually identical, although above $\sim 10^{-6}$ mm/cycle, growth rates in the silicone oils are approximately 2.5 times slower than in moist air* (Fig. 4).

The specific influence of oil viscosity can also be seen with reference to Figs. 2 to 5. Although near-threshold behavior is relatively unchanged above $\sim 10^{-6}$ mm/cycle, the data for oils show the following trends at low load ratios: a) growth rates in general are faster in higher viscosity oils, b) growth rates in silicone oils are faster than those in paraffin oils, and c) crack growth is slower in both oils than in air or hydrogen. The influence of viscosity on the value of the fatigue threshold ΔK_o appears to be negligible at R = 0.75 although at R = 0.05 there is a small but finite trend of decreasing ΔK_o with increasing kinematic viscosity in both oils (Fig. 5).

The influence of viscosity on the load ratio dependence of growth rates is illustrated in Fig. 6. Although all the oils show similar increases in propagation rates with increasing R at near-threshold levels, the effect of load ratio above $\sim 10^{-6}$ mm/cycle becomes significantly more pronounced with decreasing viscosity, especially in the paraffin oil. A listing of the measured fatigue threshold ΔK_o values in the viscous environments is given in Table IV, and is compared with previous data for gaseous and aqueous environments.[9,10,46]

*Although such differences in crack growth behavior may appear small in comparison with the overall scale of the plots, the trends shown were consistently reproducible between duplicate tests.

Analysis of Fracture Surfaces

Scanning electron micrographs of representative areas of the fatigue fracture surfaces are shown in Fig. 7. At near-threshold levels, fracture morphology in all oils was similar, showing a fine-scale transgranular mode with isolated intergranular facets, characteristic of lower strength steels tested close to ΔK_o (Fig. 7a).[6-10,15] At higher growth rates, i.e., above $\Delta K \sim 15$ MPa$\sqrt{m}$, however, fracture surface in the silicone oils contained more noticeable evidence of intergranular facets at R = 0.05 (Fig. 7b and c), although a large proportion of such facets were apparent in both oils at R = 0.75 (Fig. 7d and e).

The extent of crack surface oxidation, determined using Ar^+ sputtering Auger techniques,[10] is shown in Fig. 8 for the 5 and 12,500 cS silicone oils and the 25 cS paraffin oil. Here the thickness of the excess oxide layer (identified using ESCA to be predominately Fe_2O_3) is plotted against crack length and crack growth rate, and results compared with previous data[9,10] for moist air. Although the extent of the crack surface oxide films in moist air is inversely related to the growth rate, reaching maximum thicknesses (s) near ΔK_o of the order of 200 nm (2000 Å),[10] in oil the oxide films were uniformly much smaller and were estimated to be of the order of 3 nm (30 Å) thick.

5. DISCUSSION

Similar to previous studies on the role of gaseous and aqueous environments in influencing fatigue crack propagation in lower strength steels,[45,46] it is clear from the present work that the effect of the viscous environment is markedly different at near-threshold as opposed to higher growth rates (i.e., above and below $\sim 10^{-6}$ mm/cycle, respectively). Specifically, both dehumidified silicone and paraffin oils give rise to **faster** growth rates at near-threshold levels and **slower** growth rates above 10^{-6} mm/cycle, compared to crack growth in moist air at R = 0.05. In fact, crack propagation behavior in these oils is similar to that in dry gaseous hydrogen or helium at near-threshold levels, and yet significantly slower than in gaseous hydrogen at higher growth rates.

In general terms, such contrasting effects of environment have been rationalized in terms of a competition between two concurrent but mutually competitive processes, namely corrosion fatigue mechanisms, e.g., hydrogen embrittlement and/or active path corrosion, which **increase** crack growth rates, and crack closure mechanisms, e.g., resulting from oxidation products at the crack tip (oxide-induced) or irregular fracture morphologies (roughness-induced), which **decrease** crack growth rates.[12,48] Whereas corrosion fatigue mechanisms tend to dominate environmentally-influenced crack growth behavior at higher growth rates and at high load ratios, the role of closure mechanisms becomes increasingly more important at low load ratios as growth rates approach threshold levels. In fact, in lower strength steels, such as

the present 2.25Cr-1Mo steel, tested at the high frequencies (i.e., 50 Hz) commonly utilized for low growth rate testing, the contribution to crack advance from corrosion fatigue mechanisms, such as hydrogen embrittlement and active path corrosion, is generally fairly minimal below $\sim 10^{-6}$ mm/cycle in environments such as water, moist air, gaseous hydrogen, etc.,[45] such that closure phenomena, particularly oxide-induced closure, often dominate overall near-threshold behavior.[6-10,48]

Accordingly, near-threshold crack growth rates have been found to be faster at low load ratios in dry environments (e.g., dehumidified gaseous hydrogen, helium and oxygen) compared to moist environments (e.g., room air and wet gaseous hydrogen),[6-10] whereas behavior is similar at high load ratios where the influence of closure is minimal.* Above $\sim 10^{-6}$ mm/cycle, on the other hand, conventional corrosion fatigue processes begin to dominate such that growth rates become slower in dry inert environments, such as helium gas, compared to aggressive environments such as hydrogen gas or water vapor.[45,49]

In the present study on viscous environments, the observed effects of dehumidified oils tested at a frequency of 50 Hz can be interpreted in terms of similar considerations,** only now specifically involving three distinct mechanisms, i.e., i) exclusion of moisture from the

---

*In more oxidizing environments, sufficient crack surface corrosion deposits can form as a result of thermal oxidation, even at high load ratios where fretting effects are generally minimal, to enhance oxide-induced closure over a wider range of R.[46]

**Studies of near-threshold fatigue crack growth at ultrasonic frequencies up to 21 kHz are often conducted in oils to simulate inert environments, although the specific role of the viscous fluid contained within the crack at such high frequencies has not been documented.[50,51]

crack tip thereby minimizing hydrogen embrittlement/metal dissolution processes, ii) exclusion of moisture and oxygen from crack tip thereby minimizing oxide-induced crack closure, and iii) partial penetration of the oil films within the crack to create additional closure from the hydrodynamic wedge effect of the viscous fluid. Each mechanism is now discussed in turn.

Minimization of Hydrogen Embrittlement/Active Path Corrosion

As both dry silicone and paraffin oils do not chemically react with steel, the principal function of such media is to act as an inert environment for crack growth, as evidenced by the fact that behavior in the oils is similar to that in dry gaseous helium (Fig. 2 and 3). This is consistent with the studies of Ryder et al.[23] in Al-Zn-Mg alloys where the decreased Stage II fatigue crack growth rates measured in silicone oil were attributed to limiting the access of air to the crack tip region. This exclusion of moisture and oxygen from the vicinity of the crack tip, resulting from immersion in dehumidified oil, will thus minimize any enhancement in crack growth rates due to metal dissolution (oxidation) at the crack tip and/or hydrogen embrittlement from the consequent release of hydrogen. This is substantiated by the Auger data in Fig. 8 which show almost negligible levels of crack surface oxidation products for the oil environments at both near-threshold and higher stress intensity ranges. This reduced contribution to crack advance from corrosion fatigue processes will be effective over the entire range of growth rates and load ratios, but will dominate behavior above $\sim 10^{-6}$ mm/cycle since closure mechanisms here are less

effective. Thus it is to be expected that crack growth rates in oil in this regime will be slower than in moist air or hydrogen gas, and be comparable with rates in helium, as shown experimentally in Figs. 2 and 3. Similar explanations in terms of shielding the crack tip from detrimental environmental species have been used in the past to account for the reduction of crack growth rates in several alloys tested in inert liquid environments such as dodecyl alcohol, oils and grease, where either the inert liquid forms a physical barrier, or in the case of dodecyl alcohol forms organic oleophobic films, which exclude the presence of oxygen and water vapor from the crack tip region.[23,52]

Minimization of Oxide-Induced Crack Closure

For the current steel tested at 50 Hz, the exclusion of moisture and oxygen afforded by the oil environment has the reverse effect, however, on lower growth rates. Observations of faster near-threshold propagation rates in oil than in moist air at R = 0.05 (Figs. 2 and 3) can be attributed to a much reduced role of oxide-induced crack closure in the oil environments due to far less crack surface oxidation. Such corrosion debris, which forms as a result of fretting oxidation between the crack walls,[5-10] is about 20 to 40 times thicker in moist air compared to inert oil environments (Fig. 8). This results in significant closure near ΔK_o in moist air since the oxide films here become comparable in size to the crack tip opening displacements. At high load ratios, however, where fretting and closure effects are minimal, near-threshold behavior in the air and oil environments becomes very similar (Fig. 4).

The relative effect of oxide-induced crack closure on near-threshold growth rates in dry oil and in moist air (at R = 0.05) can be appreciated by considering the simple model of a rigid wedge inside a linear elastic crack.[10] The model considers the reduction in stress intensity range from its nominal value ($\Delta K = K_{max} - K_{min}$) to some near tip effective value ($\Delta K_{eff} = K_{max} - K_{cl}$), and estimates the closure stress intensity, K_{cl}, in terms of the maximum oxide wedge thickness s located at distance, 2ℓ, behind the crack tip:

$$K_{cl} \approx \frac{sE}{4\sqrt{\pi\ell}\,(1 - \nu^2)} \quad , \qquad (1)$$

where $E/(1 - \nu^2)$ is the effective elastic modulus in plane strain.[10] With $\ell \sim 2$ μm,[10,53] the peak excess oxide thickness, s, in moist air close to ΔK_o can be seen to be ~ 200 nm compared to ~ 3 nm oil (Fig. 8). From Eq. (1) the corresponding values of the closure stress intensity K_{cl} at R = 0.05 are ~ 4.5 MPa$\sqrt{m}$ in moist air and less than 0.1 MPa$\sqrt{m}$ in oil. Thus at a nominal ΔK of 8 MPa$\sqrt{m}$, roughly half of the applied stress intensity range in air is lost to closure, whereas less than 1 pct is affected in oil. This clearly indicates that the driving force for crack extension in oil is far less restricted by oxide-induced closure. Similar calculations show closure effects to be negligible in both the oil and moist air at R = 0.75.

Role of Viscous Fluid-Induced Crack Closure

Both effects of the oil environments described above, in terms of minimizing corrosion fatigue mechanisms and oxide-induced closure, are

essentially independent of oil chemistry and viscosity, provided the oil is chemically inert. However, the current low load ratio results in Figs. 2 to 7 indicate growth rates to be somewhat higher in the higher viscosity oils, particularly above $\sim 10^{-6}$ mm/cycle, although the effect saturates above 12,500 cS. Moreover, at comparable viscosities, paraffin oils show the faster growth rates near ΔK_o and the slower growth rates above $\sim 10^{-6}$ mm/cycle (at R = 0.05). Such observations can be rationalized by considering the additional crack closure which arises due to the hydrodynamic wedging action of a viscous fluid within the crack walls.

As modelled in Part II of this paper,[26] the description of this closure phenomenon and its role in governing the effect of oil viscosity on growth rates must include an analysis of both the extent of oil penetration and the subsequent oil pressure created within the crack. Earlier models[20,21,41] of this phenomenon have generally ignored the kinetics of oil penetration, yet both the extent of penetration and the internal oil pressure are important since they have opposite dependencies on viscosity.[22]

In the present model of viscous fluid-induced closure,[26] the kinetics of oil penetration are assessed in terms of Newman's capillary flow equations,[44] where the extent of oil penetration (d) into the crack of length (a) after time (t) is given by:

$$d^2(t) = \left[\frac{\gamma \cos\beta}{3\eta\rho}\right] \int_0^t \langle h \rangle dt \qquad (2)$$

where $\langle h \rangle$ is the average crack opening width, γ the surface tension of

the oil, β the wetting angle between fluid and crack wall, η the kinematic viscosity and ρ the density. The resulting hydrodynamic pressure distribution p(x), distance x along an edge crack in an infinite plate, is then estimated from the analysis of Endo et al.[20,21] for the fully penetrated crack (i.e., d/a = 1), or from the analysis by Fuller[54] of fluids between parallel plates for the partially penetrated crack (i.e., d/a < 1), viz:

$$p(x) = 6\eta\rho\left(\frac{1}{h_m^3}\frac{dh_m}{dt}\right)a^2 \log\left(1 - \frac{x}{a}\right), \quad d/a = 1, \quad x/a \leq 1, \qquad (3a)$$

or

$$p(x) = 6\eta\rho\left(\frac{1}{\langle h\rangle^3}\frac{d\langle h\rangle}{dt}\right) x(d - x), \quad d/a < 1, \quad x/d \leq 1, \qquad (3b)$$

where h_m is the opening width at the crack mouth and dh/dt is the closing velocity of the crack walls.[26] Using superposition methods to compute the maximum resultant linear elastic stress intensity arising from such oil pressure (K^*_{max}), the effective stress intensity range corrected for viscous fluid-induced closure becomes:

$$\Delta K_{eff} = K_{max} - (K_{min} + K^*_{max}) \quad . \qquad (4)$$

With such analyses it is apparent that the extent of such closure should progressively increase with increasing viscosity although at very high viscosities, values of K^*_{max} will be kinetically limited by

the ability of the oil to penetrate into the crack. Thus, where the rate of oil penetration ($\dot{d}$) (from Eq. 2) exceeds the rate of crack extension ($\dot{a}$), the full penetration model becomes appropriate and growth rates are to be expected to be lower in higher viscosity oils, as originally observed by Endo et al.[20,21] However, where $\dot{d}$ is less than $\dot{a}$, e.g., with increasing ΔK levels in higher viscosity oils, the proposed partial penetration model (Eqs. 2 and 3b) must be used, and the resulting dependency of K^*_{max}, and hence growth rates, on viscosity will be a function of the relative magnitude of the hydrodynamic and kinetic effects. As described in detail in Part II,[26] the lowest growth rates, between $\sim 10^{-6}$ to 10^{-4} mm/cycle, observed in the paraffin oils (Fig. 3) can be quantitatively ascribed to rapid oil penetration (due in part to a 69 pct increase in surface tension over the silicone oils) and resulting higher K^*_{max} values, whereas the highest growth rates in the 12,500 and 60,000 cS silicone oils (Fig. 2) appear to result from restricted oil penetration and hence lower K^*_{max} values with the highly viscous fluids.

The concept of viscous fluid-induced closure is also pertinent to explaining the varying dependency of growth rates on load ratio in the various oil environments, particularly above $\sim 10^{-6}$ mm/cycle (Fig. 6). Although the influence of load ratio is generally relatively insignificant between $\sim 10^{-6}$ to 10^{-3} mm/cycle, except in the presence of major environmentally-assisted mechanisms, it is clear that the role of the load ratio in the oil environments becomes progressively more prominant as the viscosity is decreased, and is particularly marked in the 25 cS paraffin oil. In terms of the current analysis, both the oil

penetration distance (d) and the resultant stress intensity K^*_{max} due to the internal oil pressure are complex functions of R. However, although the value of K^*_{max} would be expected to decrease with increasing load ratio, the increased crack opening promotes far greater oil penetration into the crack. Accordingly, there is little effect of R with high viscosity oils (see Fig. 6c for 60,000 cS silicone oil) due to restricted oil penetration. Conversely, with lower viscosity and paraffin oils (Fig. 6a and d) the enhanced oil penetration yields a fluid-induced closure which is only effective at the small crack opening associated with low load ratio conditions. Quantitative predictions for the extent of such closure are derived in ref. 26.

Thus, the observed effects of oil chemistry and viscosity on fatigue crack propagation behavior can be rationalized in terms of a mutual competition between corrosion fatigue mechanisms, crack closure and hydrodynamic wedging processes. Although the magnitude of the differences in growth rate behavior in the various viscous fluids is not large, for the conditions investigated, the current analysis suggests dehumidified inert oil environments tend i) to suppress moisture-induced hydrogen embrittlement/metal dissolution processes (leading to **slower** growth rates than in moist air **above** $\sim 10^{-6}$ mm/cycle), ii) to suppress similarly oxide-induced crack closure (leading to **faster** growth rates than in moist air **below** $\sim 10^{-6}$ mm/cycle) and iii) to promote viscous fluid-induced crack closure (leading to a complex dependency of growth rates on viscosity).

6. CONCLUSIONS

Based on a study of the effect of dehumidified viscous environments on the room temperature fatigue crack propagation behavior of a bainitic 2.25Cr-1Mo steel, specifically involving silicone and paraffin oils of viscosities ranging from 5 to 60,000 cS, the following conclusions can be made:

1) Dehumidified silicone and paraffin oil environments were found to have significant but opposite effects on fatigue crack propagation above and below $\sim 10^{-6}$ mm/cycle.

2) At R = 0.05 in the near-threshold regime (da/dN $\lesssim 10^{-6}$ mm/cycle), growth rates in dry oil were **higher** than those in moist air by up to two orders of magnitude with fatigue threshold ΔK_o values approximately 30 pct lower, although at R = 0.75, behavior was virtually identical.

3) At higher propagation rates above $\sim 10^{-6}$ mm/cycle, growth rates at R = 0.05 and 0.75 in dry oil were **lower** than those in moist air by up to an order of magnitude and comparable with those for dry gaseous helium.

4) At low load ratios, crack growth rates in both oils tended to increase with increasing oil viscosity, although the effect was diminished above above 12,500 cS and at lower, near-threshold growth rates.

5) The complex dependence of fatigue crack propagation behavior on dehumidified viscous environments is rationalized in terms of three mutually competitive mechanisms: suppression of moisture-related

corrosion fatigue processes (i.e., hydrogen embrittlement and/or active path corrosion), minimization of oxide-induced crack closure, and development of additional closure through a hydrodynamic action caused by the penetration of the oil inside the crack. A quantitative model for the latter phenomenon is described in Part II of this paper.

Acknowledgements - The work was supported by the Director, Office of Energy Research, Office of Basic Energy Sciences, Materials Science Division of the U.S. Department of Energy under Contract No. DE-AC03-76SF00098. Thanks are due to Don Krieger for experimental assistance and to the Dow Corning Corporation and Fisher Scientific Company for supplying the oils.

NOMENCLATURE

a	crack length
B	test piece thickness
d	penetration distance of viscous fluid into an edge crack
da/dN	fatigue crack growth rate per cycle
E	elastic (Young's) modulus
$h, \langle h \rangle, h_m$	instantaneous, average and crack mouth opening width, respectively
K	linear elastic stress intensity factor in Mode I
K_{cl}	stress intensity to cause closure of the crack
K_{Ic}	plane strain fracture toughness (Mode I)

K_{Iscc}	threshold stress intensity for hydrogen-assisted cracking
K_{max}, K_{min}	maximum and minimum intensities, respectively, during fatigue cycle
K^*_{max}	stress intensity due to hydrodynamic action of viscous fluid inside crack, evaluated at peak loads
ΔK	alternating stress intensity ($K_{max} - K_{min}$)
ΔK_{eff}	effective stress intensity range ($K_{max} - K_{cl}$)
ΔK_o	threshold stress intensity range for no growth of a long crack
ℓ	half distance between the peak oxide thickness and crack tip
N	number of cycles
p(x)	pressure distribution as a function of distance x along crack
r_Δ	cyclic plastic zone size
R	load ratio (K_{min}/K_{max})
s	excess oxide thickness measured on fracture surface
UTS	ultimate tensile strength
t	time
x	variable denoting distance along crack, measured from crack mouth
β	wetting angle
γ	surface tension of fluid
η	kinematic viscosity
ν	Poisson's ratio

ρ	density of fluid
σ_y	yield strength

REFERENCES

1. S. Suresh and R. O. Ritchie: in Fatigue Crack Growth Threshold Concepts, D. L. Davidson and S. Suresh, eds., The Metallurgical Society of AIME, Warrendale, PA, 1984, in press (Lawrence Berkeley Laboratory Report No. LBL-16263, Sept. 1983).
2. W. Elber: in Damage Tolerance in Aircraft Structures, ASTM STP 486, American Society for Testing and Materials, Philadelphia, PA, 1971, p. 230.
3. S. Suresh and R. O. Ritchie: Int. Met. Reviews, 1984, vol. 25, in press (University of California, Berkeley, Report No. UCB/RP/83/A1014, June 1983).
4. B. Budiansky and J. W. Hutchinson: J. Appl. Mech., Trans. ASME Series E, 1978, vol. 45, p. 267.
5. K. Endo, K. Komai and Y. Matsuda: Memo Fac. Eng., Kyoto Univ., 1969, vol. 31, p. 25.
6. R. O. Ritchie, S. Suresh and C. M. Moss: J. Eng. Mat. Tech., Trans. ASME Series H, 1980, vol. 102, p. 293.
7. A. T. Stewart: Eng. Fract. Mech., 1980, vol. 13, p. 463.
8. H. Kitagawa, S. Toyohira and K. Ikeda: in Fracture Mechanics in Engineering Applications, G. C. Sih and S. R. Valluri, eds., Sijthoff and Noordhoff, The Netherlands, 1981.
9. S. Suresh, G. F. Zamiski and R. O. Ritchie: Metall. Trans. A, 1981, vol. 12A, p. 1435.
10. S. Suresh, D. M. Parks and R. O. Ritchie: in Fatigue Thresholds, J. Bäcklund, A. Blom and C. J. Beevers, eds., EMAS Publ. Ltd., Warley, U.K., 1982, vol. 1, p. 391.

11. P. K. Liaw, T. R. Leax, R. S. Williams and M. G. Peck: Metall. Trans. A, 1982, vol. 13A, p. 1607.

12. A. K. Vasudēvan and S. Suresh: Metall. Trans. A, 1982, vol. 13A, p. 2271.

13. S. Purushothamon and J. K. Tien: in Strength of Metals and Alloys, (ICSMA-5 Conf. Proc.), P. Haasen et al., eds., Pergamon Press, New York, 1979, vol. 2, p. 1267.

14. N. Walker and C. J. Beevers: Fat. Eng. Matls. Struct., 1979, vol. 1, p. 135.

15. K. Minakawa and A. J. McEvily: Scripta Met., 1981, vol. 15, p. 633.

16. R. O. Ritchie and S. Suresh: Metall. Trans. A, 1982, vol. 13A, p. 937.

17. S. Suresh and R. O. Ritchie: Metall. Trans. A, 1982, vol. 13A, p. 1627.

18. G. T. Gray, A. W. Thompson and J. C. Williams: Metall. Trans. A, 1983, vol. 14A, p. 421.

19. K. Esaklul, A. G. Wright and W. W. Gerberich: Scripta Met., 1983, vol. 17, p. 1073.

20. K. Endo, T. Okada and T. Hariya: Bull. JSME, 1972, vol. 25, p. 439.

21. K. Endo, T. Okada, K. Komai and M. Kiyota: Bull. JSME, 1972, vol. 15, p. 1316.

22. J.-L. Tzou, S. Suresh and R. O. Ritchie: in Mechanical Behaviour of Materials - IV, Proc. 4th Intl. Conf. (ICM-4), Stockholm, Sweden, J. Carlsson and N. G. Ohlson, eds., Pergamon Press, New York, 1983, vol. 2, p. 711.

23. D. A. Ryder, M. Martin and M. Abdullah: Metal. Sci., 1977, vol. 11, p. 340.

24. O. Vosikovsky: Corrosion, 1976, vol. 32, p. 472.

25. O. Vosikovsky and A. Rivard: Corrosion, 1982, vol. 38, p. 19.

26. J.-L. Tzou, C. H. Hsueh, A. G. Evans and R. O. Ritchie: (Part II), Acta Met., 1983, in review (Lawrence Berkeley Laboratory Report No. LBL-16842, Dec. 1983).

27. C. J. Polk, W. R. Murphy and C. N. Rowe: ASLE Trans., 1975, vol. 18, p. 290.

28. N. E. Frost: Appl. Matls. Res., 1964, vol. 3, p. 131.

29. L. Grunberg and D. Scott: J. Inst. Petrol., 1958, vol. 44, p. 406.

30. P. Schatzberg and I. M. Felson: Wear, 1968, vol. 12, p. 331.

31. J. A. Ciruna and H. J. Szieleit: Wear, 1973, vol. 24, p. 107.

32. C. J. Polk and C. N. Rowe: ASLE Trans., 1976, vol. 29, p. 23.

33. R. E. Cantley: ASLE Trans., 1977, vol. 20, p. 244.

34. M. E. Otterbein: ASLE Trans., 1958, vol. 1, p. 33.

35. W. J. Anderson and T. L. Carter: ASLE Trans., 1958, vol. 1, p. 266.

36. J. B. Martin and A. Cameron: J. Mech. Eng. Sci., 1961, vol. 3, p. 148.

37. F. G. Rounds: ASLE Trans., 1962, vol. 5, p. 172.

38. W. E. Littmann, R. L. Widner, J. O. Wolfe and J. D. Stover: J. Lub. Tech., Trans. ASME Series F, 1968, vol. 90, p. 89.

39. F. G. Rounds: J. Lub. Tech., Trans. ASME Series F, 1971, vol. 93, p. 236.

40. F. G. Rounds: ASLE Trans., 1977, vol. 20, p. 115.

41. G. D. Galvin and H. Naylor: Proc. Instn. Mech. Engrs., 1964-65, vol. 179, p. 857.

42. I. Koved: ASLE Trans., 1966, vol. 9, p. 222.

43. S. Way: J. Appl. Mech., Trans. ASME Series E, 1935, vol. 2, p. A49.

44. S. Newman: J. Colloid Interface Sci., 1968, vol. 26, p. 209.

45. S. Suresh and R. O. Ritchie: Metal Sci., 1982, vol. 16, p. 529.

46. S. Suresh and R. O. Ritchie: Eng. Fract. Mech., 1983, vol. 18, p. 785.

47. R. O. Ritchie: Int. Met. Reviews, 1979, vol. 20, p. 205.

48. R. O. Ritchie, S. Suresh and P. K. Liaw: in Ultrasonic Fatigue, J. M. Wells et al., eds. The Metallurgical Society of AIME, Warrendale, PA, 1982, p. 443.

49. R. C. Brazill, G. W. Simmons and R. P. Wei: J. Eng. Mat. Tech., Trans. ASME Series H, 1979, vol. 101, p. 129.

50. B. Weiss, R. Stickler, J. Fembock and K. Pfaffinger: Fat. Eng. Matls. Struct., 1979, vol. 2, p. 73.

51. S. E. Stanzl and E. K. Tschegg: Acta Met., 1981, vol. 29, p. 21.

52. W. L. Holshouser and H. P. Utech: Proc. ASTM, 1961, vol. 61, p. 749.

53. S. Suresh and R. O. Ritchie: Scripta Met., 1983, vol. 17, p. 575.

54. D. D. Fuller, in Theory and Practice of Lubrication for Engineers, Wiley, New York, 1956, p. 134.

Table I: Chemical Composition in Wt Pct of 2¼Cr-1Mo Steel (A542-3)

C	Mn	Si	Ni	Cr	Mo	Cu	P	S
0.12	0.45	0.21	0.11	2.28	1.05	0.12	0.014	0.015

Table II: Room Temperature Mechanical Properties of 2¼Cr-1Mo Steel (A542-3)

Yield Strength								
Monotonic	Cyclic[1]	UTS	Elong.[2]	Redn. Area	Charpy Impact Energy	K_{Ic}[3]	K_{Iscc}[4]	
(MPa)	(MPa)	(MPa)	(Pct)	(Pct)	(J)	(MPa$\sqrt{m}$)	(MPa$\sqrt{m}$)	
500	400	610	25	77	197	295	85	

[1] Measured from incremental step tests

[2] On a 45 mm gauge length

[3] Computed from J_{Ic} measurements

[4] Based on slowly rising load test in 138 kPa hydrogen gas

Table III: Room Temperature Physical Properties of the Silicone and Paraffin Oils Investigated

Oil	Kinematic Viscosity (η) (cS)	Density (ρ) (gm/cm^3)	Surface Tension (γ) (dyne/cm)
Silicone Oil	5	0.920	19.7
	1,000	0.971	21.2
	12,500	0.975	21.5
	60,000	0.975	21.5
Paraffin Oil	25	0.870	35.0
	75	0.890	36.0

Table IV: Experimental Fatigue Threshold Data for A542 Steel Tested at 50 Hz at R = 0.05 and 0.75.

Environment	Threshold Stress Intensity Range (ΔK_o) R = 0.05 ($MPa\sqrt{m}$)	R = 0.75 ($MPa\sqrt{m}$)
5 cS silicone oil	6.4	2.8
1,000 cS silicone oil	6.1	3.0
12,500 cS silicone oil	5.8	3.0
60,000 cS silicone oil	5.7	3.0
25 cS paraffin oil	5.9	3.0
75 cS paraffin oil	5.2	-
moist air*	7.7	3.2
dry hydrogen gas*	5.2	3.3
dry helium gas*	6.2	-
distilled water*	7.8	5.4

*Data from refs. 9 and 46.

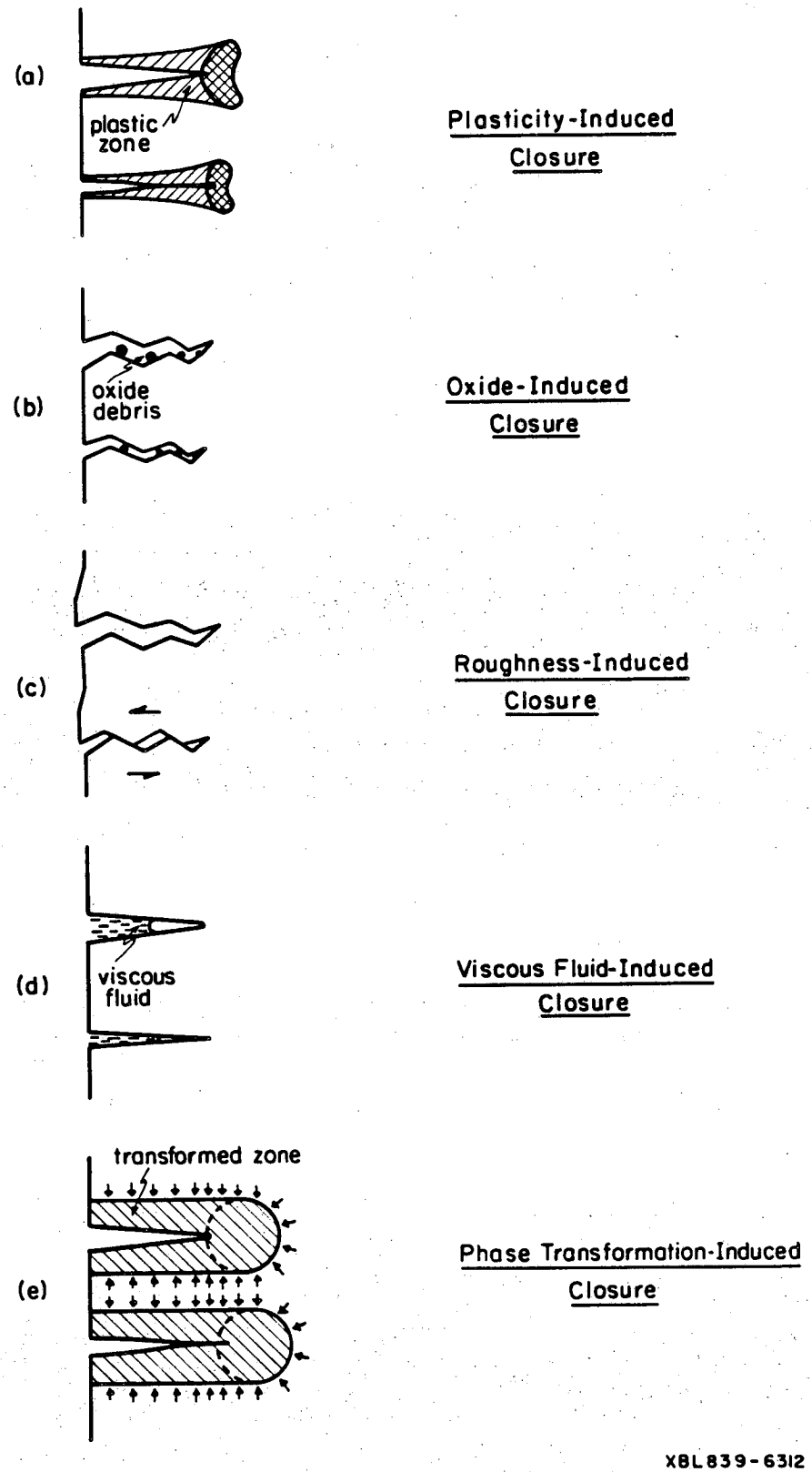

Fig. 1: Schematic illustrations of mechanisms of fatigue crack closure (after ref. 1).

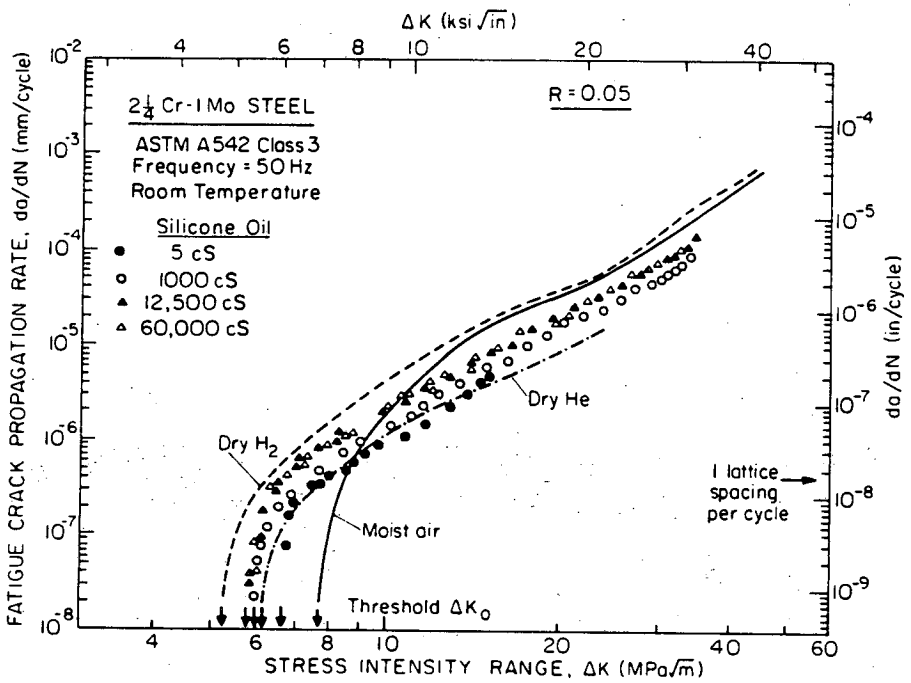

XBL 832-5311(a)

Fig. 2: Variation of fatigue crack propagation rates (da/dN) with ΔK in bainitic 2¼Cr-1Mo steel tested at R = 0.05 in 5, 1,000, 12,500 and 60,000 cS silicone oils. Results compared with previous data (ref. 9) for gaseous environments of moist air, dry hydrogen and dry helium.

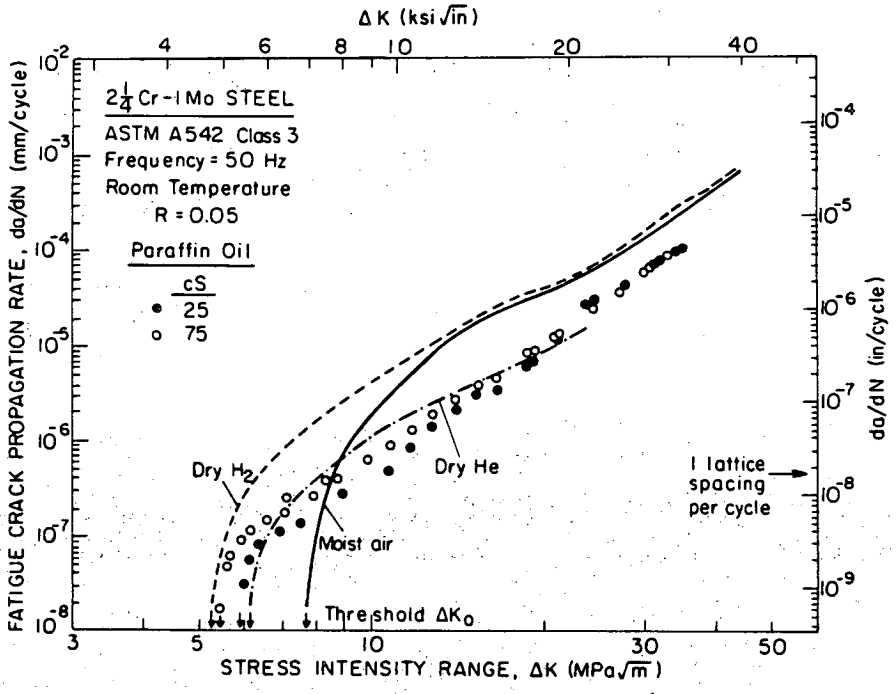

XBL 832-5311(b)

Fig. 3: Variation of fatigue crack propagation rates (da/dN) with ΔK in bainitic 2¼Cr-1Mo steel tested at R = 0.05 in 25 and 75 cS paraffin oils. Results compared with previous data (ref. 9) for gaseous environments of moist air, dry hydrogen and dry helium.

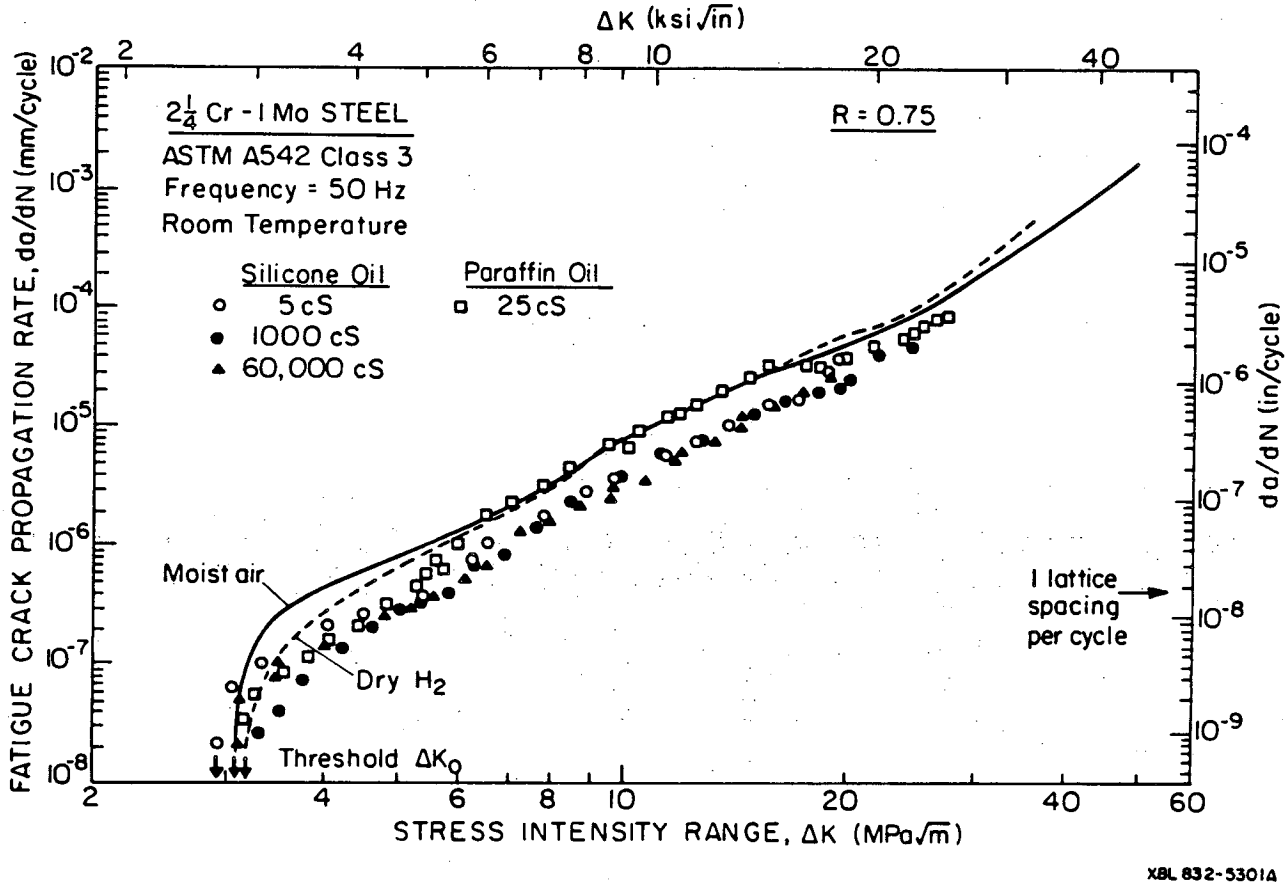

Fig. 4: Variation of fatigue crack propagation rates (da/dN) with ΔK in bainitic 2¼Cr-1Mo steel tested at R = 0.75 in silicone and paraffin oils. Results compared with previous data (ref. 9) for moist air and dry hydrogen gas.

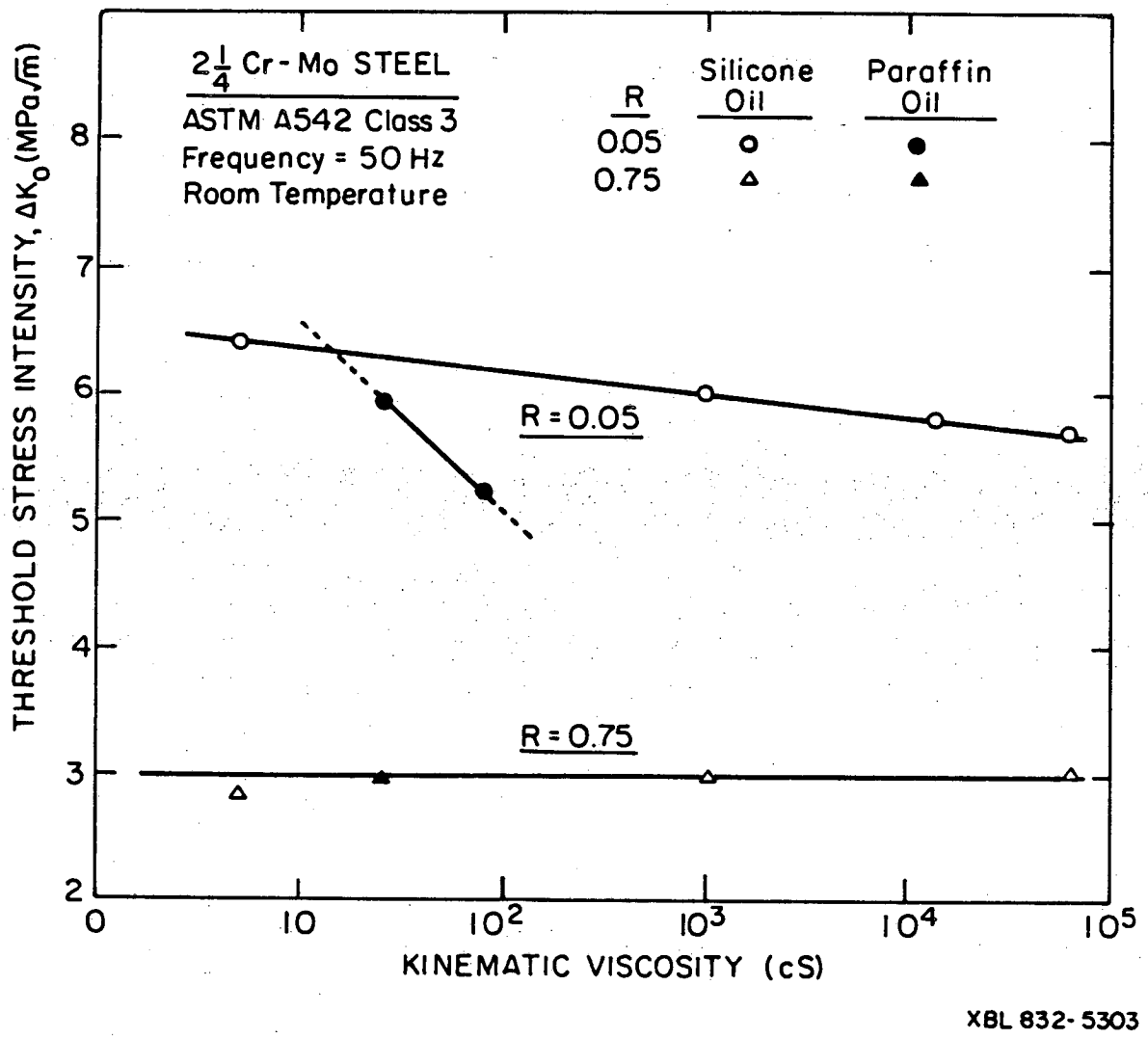

Fig. 5: Variation of fatigue threshold stress intensity range ΔK_0 with kinematic viscosity for tests in paraffin and silicone oils at load ratios of R = 0.05 and 0.75.

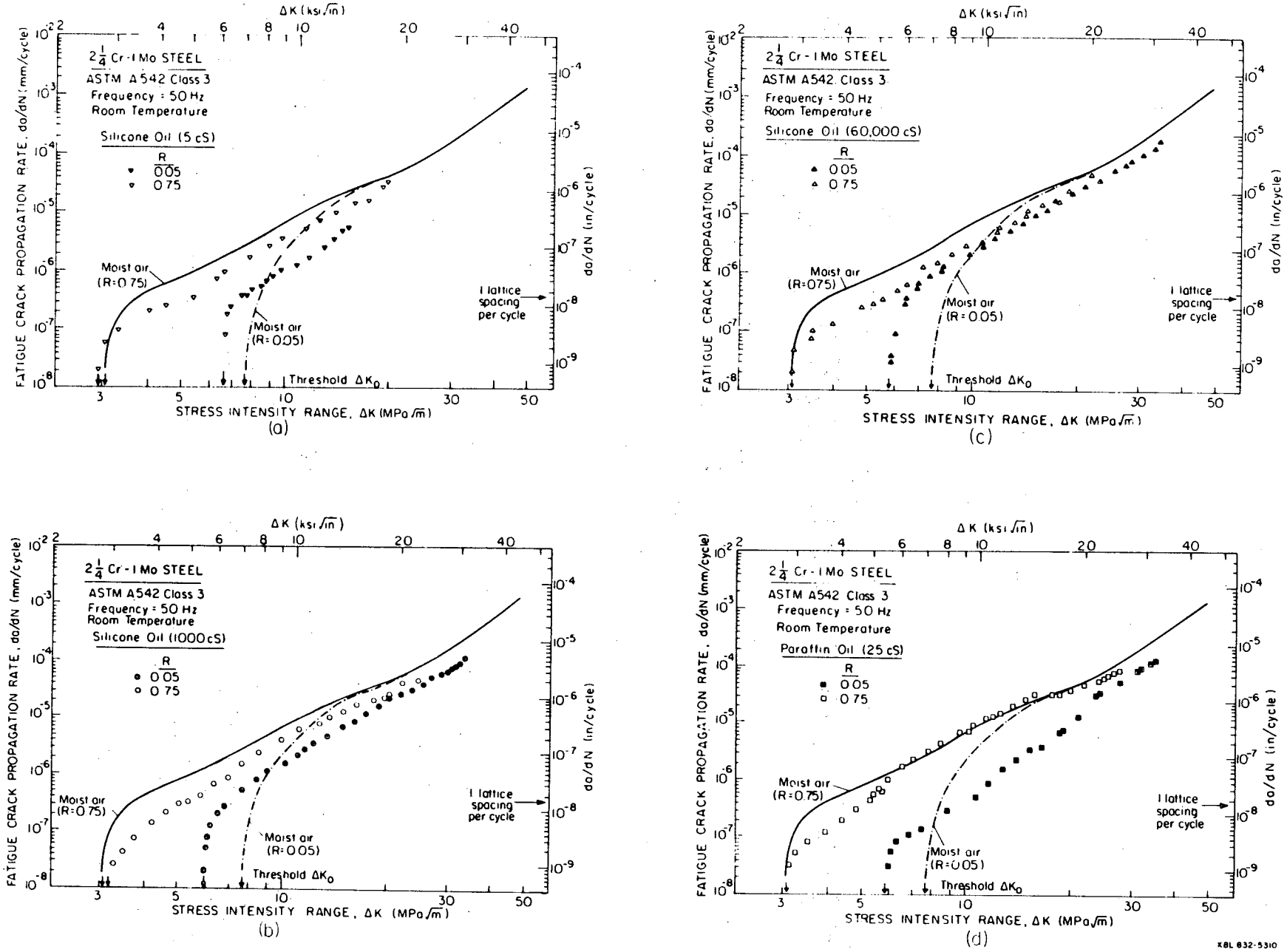

Fig. 6: Influence of oil composition and viscosity on the load ratio dependence of fatigue crack propagation behavior of bainitic 2¼Cr-1Mo steel tested in a) 5 cS silicone oil, b) 1,000 cS silicone oil, c) 60,000 cS silicone oil and d) 25 cS paraffin oil. Results compared with previous data (ref. 9) for tests at R = 0.05 and 0.75 in moist air.

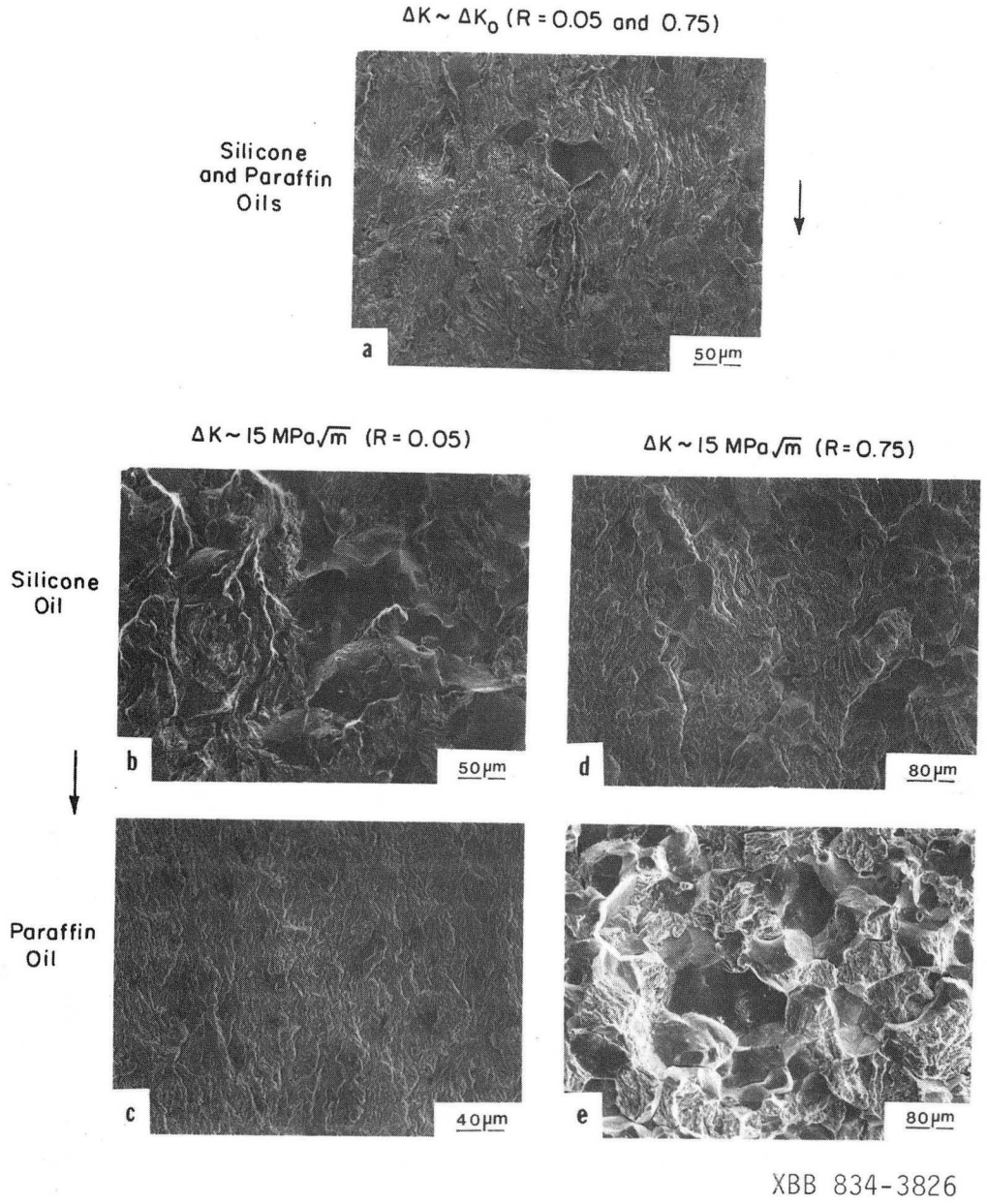

Fig. 7: Fractography of fatigue crack propagation in oil environments showing a) predominately transgranular mode, characteristic of near-threshold behavior and b-d) mixed transgranular/intergranular mode typical of higher growth rates ($\Delta K \sim 15$ MPa$\sqrt{m}$) at both low and high load ratios. Arrows indicate macroscopic direction of crack growth.

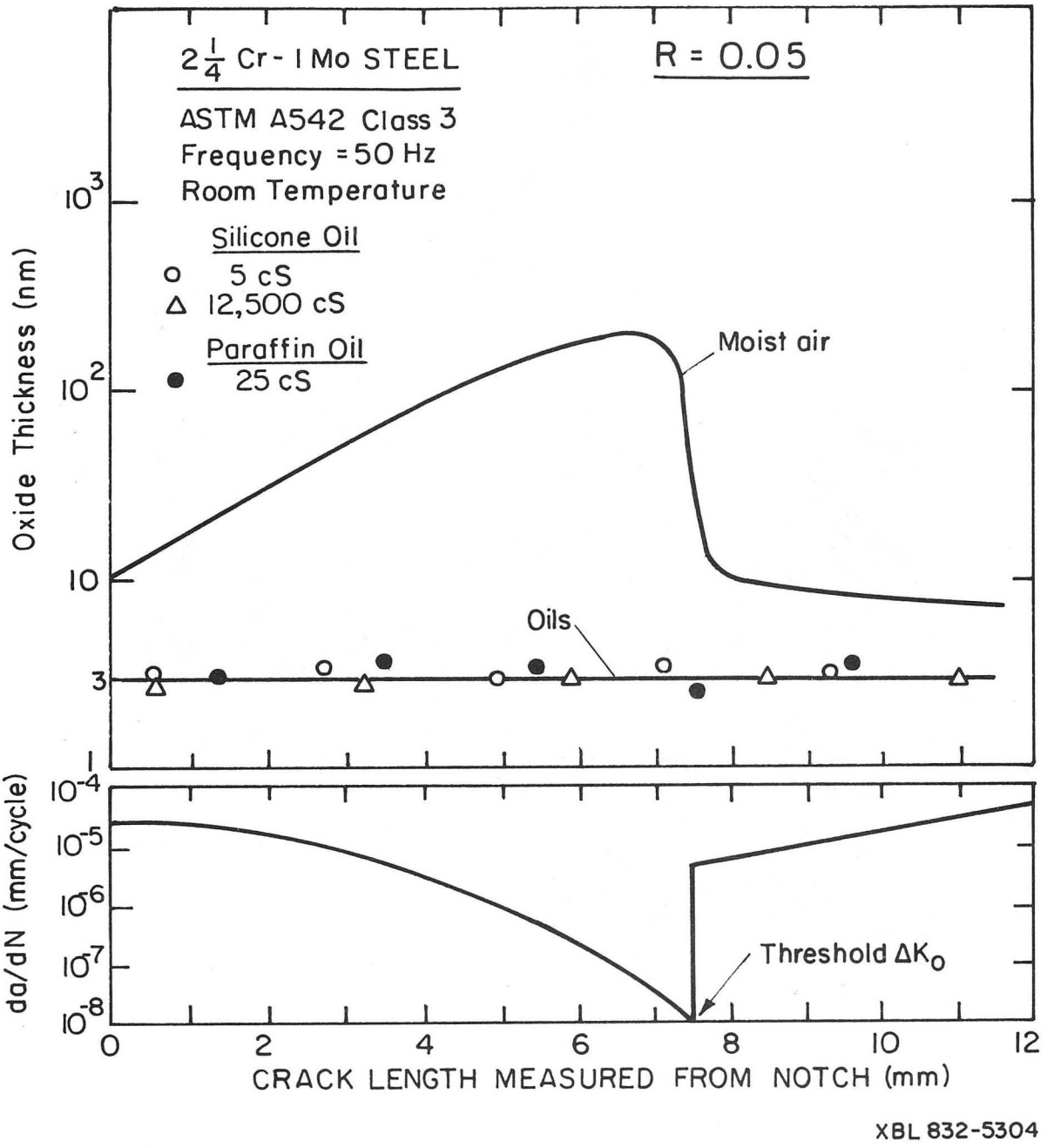

Fig. 8: Scanning Auger measurements of the excess crack surface oxide thickness (s) as a function of the length of the fatigue crack and the crack growth rate (da/dN) for bainitic 2¼Cr-1Mo steel. Data points for tests at R = 0.05 in silicone and paraffin oils are compared with previous results (ref. 9) in moist air. Auger analysis performed following Ar^+ sputtering time of 4 min at a sputter rate of 150 Å/min, using a Ta_2O_5 standard.

This report was done with support from the Department of Energy. Any conclusions or opinions expressed in this report represent solely those of the author(s) and not necessarily those of The Regents of the University of California, the Lawrence Berkeley Laboratory or the Department of Energy.

Reference to a company or product name does not imply approval or recommendation of the product by the University of California or the U.S. Department of Energy to the exclusion of others that may be suitable.

TECHNICAL INFORMATION DEPARTMENT
LAWRENCE BERKELEY LABORATORY
UNIVERSITY OF CALIFORNIA
BERKELEY, CALIFORNIA 94720